SURGE Project Report

Akshat Jain

1 Introduction

The aim of the project is to verify the Zel'dovich Curve assuming a Spherical Collapse Model and testing it on real world simulation data. In the first phase of the project, we are performing preliminary calculations to understand the density calculations and how over-density of a region might be calculated. Additionally we will try to incorporate the velocity of each particle and see how the particles interact to affect the over-density with time. Since each of the particle has a group velocity engrained in its numerical data, we will see how to extract the inflow and outflow velocity from it.

2 Numerical Analysis

For this part, we will assume a cube of length 20 units, with its center at the origin. We shall choose points in it where we will place 1 unit mass point objects. Then, creating concentric shells of varying radii, we shall calculate the overdensity for each of them.

There shall be 2 distributions of points - Random and Gaussian.

2.1 Random Distribution

We have taken N = 100000 randomly distributed within the cuboid. The number of concentric shells are 50 starting from r = 1 and going till r = 10 units, equidistant from each other.

We will calculate the spherically integrated density for each shell and plot it with respect to the shell radii.

The spherically integrated density within a radius r_i is given by:

$$\bar{\rho}(r_i) = \frac{M(< r_i)}{V(< r_i)} = \frac{M(< r_i)}{\frac{4}{3}\pi r_i^3} \tag{1}$$

where:

- $\bar{\rho}(r_i)$ is the average density within radius r_i,
- $M(< r_i)$ is the total mass enclosed within radius r_i,
- $V(< r_i) = \frac{4}{3}\pi r_i^3$ is the volume of the sphere of radius r_i.

The graphs of various iterations are shown below.

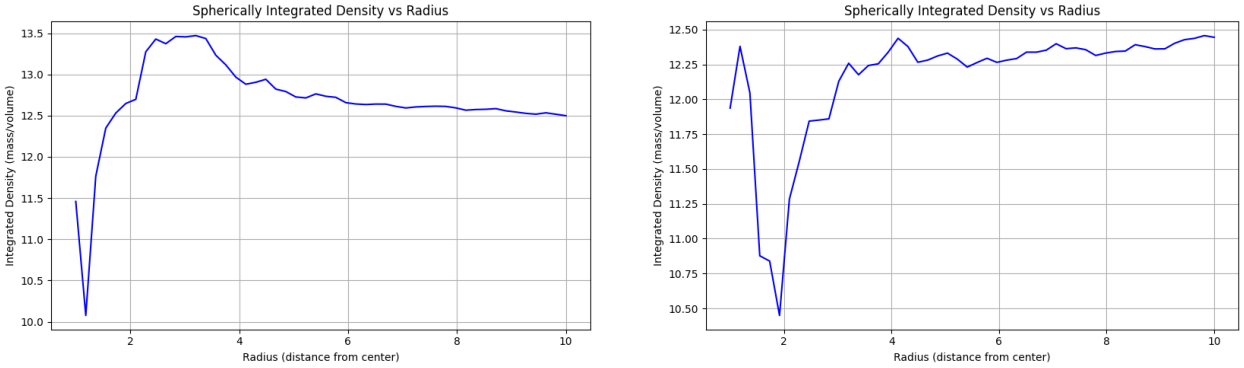

Figure 1: Comparison of two different simulation runs

To analyze the general trend and eliminate the noise for the low radii spheres, we run the simulation for 200 iterations and calculate the mean as well as standard deviation for the same. The Expected density is

also shown in the graph. Since it is a homogenous distribution, the expected density will be a constant with respect to radius, which is calculated as follows :

$$\rho_{\text{exp}} = \frac{N \cdot m}{(2L)^3} \tag{2}$$

where:

- ρ_{exp} is the expected uniform density of the cube,
- N is the total number of particles randomly distributed in the cube,
- m is the mass of each individual particle,
- $2L$ is the length of the cube's side (assuming the cube is centered at the origin and spans from $-L$ to $+L$ along each axis).

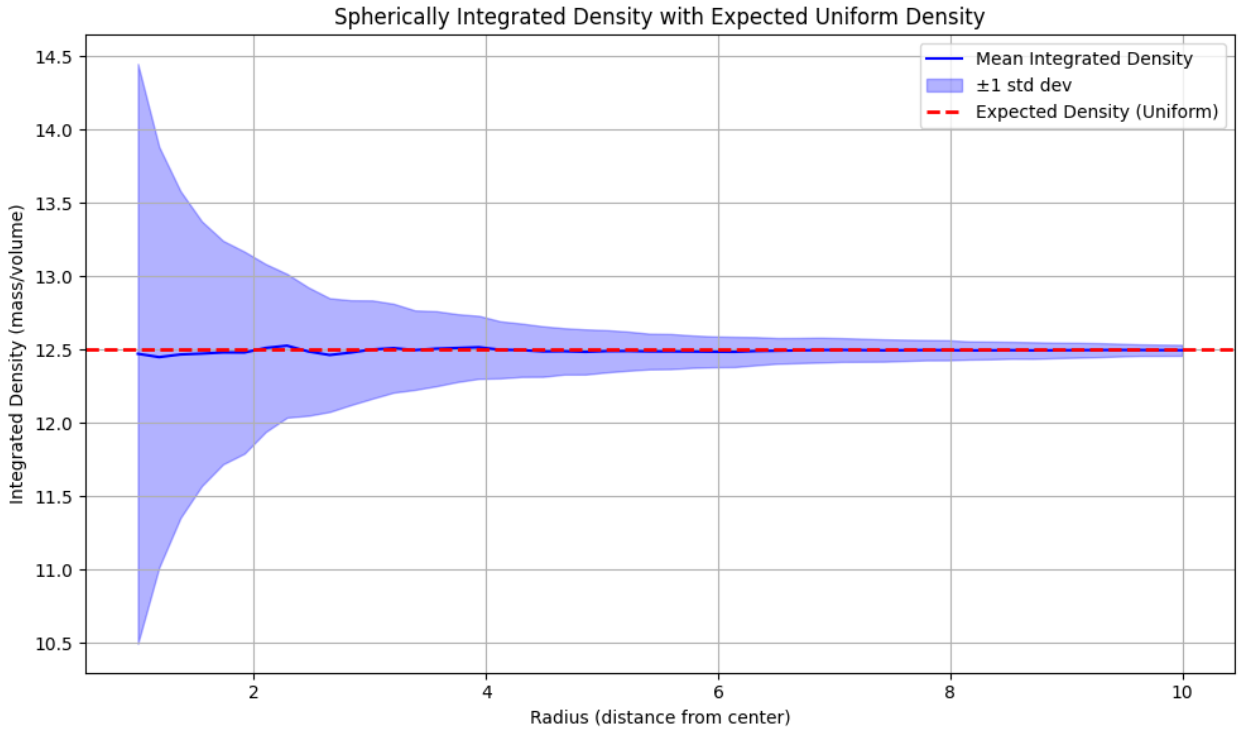

Figure 2: Error Analysis for Random Distribution

We observe that the standard deviation is very high when the radius of the shell is close to the center, which is further confirmed by Figure 1. As we move further away from the center, the standard deviation decreases and we approach the Expected Mean Density of 12.5 very close. A possible explanation for the high standard deviation, is shot noise as the number of sample points inside that region is low causing random fluctuations to have a greater noise.

To better display this, we can plot the overdensity of the region given by the formula :

$$\delta(r) = \frac{\rho(r) - \bar{\rho}}{\bar{\rho}}$$

where:

- $\delta(r)$ is the overdensity at radius r,
- $\rho(r)$ is the spherically integrated (average) density within radius r,
- $\bar{\rho}$ is the average density of the entire volume:

$$\bar{\rho} = \frac{M_{\text{total}}}{V_{\text{total}}}$$

We observe that upon increasing the number of sample points, the noise decreases.

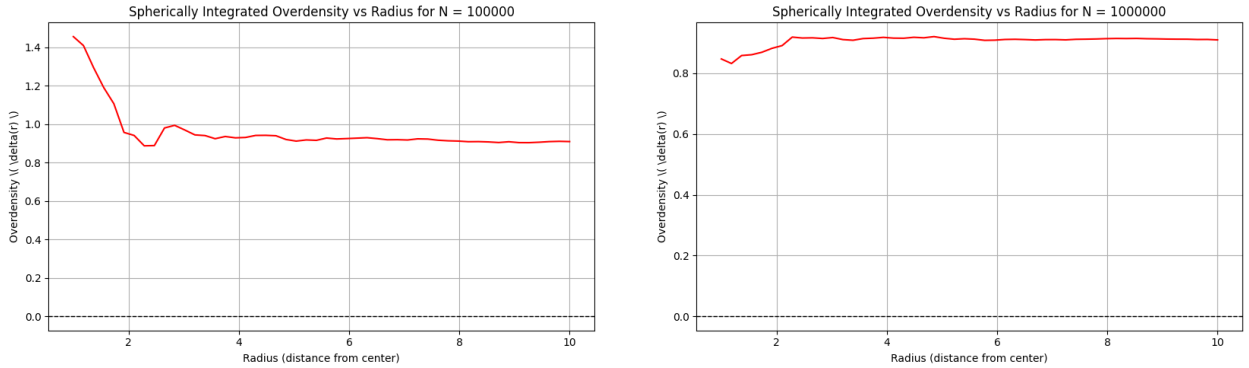

Figure 3: Results showing Decreasing Shot Noise

2.2 Gaussian Distribution

We have taken N = 100000 points within the cube. The number of concentric shells are 50 starting from r = 1 and going till r = 10 units, equidistant from each other. The standard deviation for the gaussian distribution is taken to be 3. We use the following equation to model the distribution :

$$P(r) = 4\pi r^2 \cdot \frac{1}{(2\pi\sigma^2)^{3/2}} \exp\left(-\frac{x^2+y^2+z^2}{2\sigma^2}\right)$$

We will calculate the density for each shell individually and plot it with respect to the radii. The density in each spherical shell is computed using the formula:

$$\rho(r_i) = \frac{M_i}{V_i}$$

where:

- $\rho(r_i)$ is the average density in the i-th shell,
- M_i is the total mass of particles within the shell,
- V_i is the volume of the shell:

$$V_i = \begin{cases} \frac{4}{3}\pi r_i^3 & \text{if } i = 0 \\ \frac{4}{3}\pi(r_i^3 - r_{i-1}^3) & \text{if } i > 0 \end{cases}$$

The graphs of various iterations are shown below.

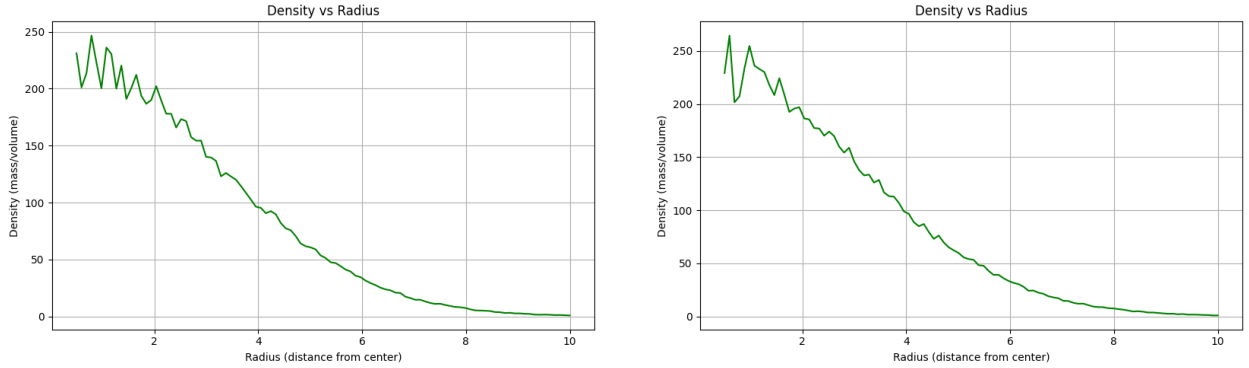

Figure 4: Comparison of two different simulation runs

We observe a similar shot noise for the shells closer to the center of the cube. We analyze the general trend, we run the simulation for 200 iterations performing similar error analysis as to the last time. For the expected density this time, we use the following formula :

$$\rho(r_i) = \frac{M_i}{V_i}$$

where:

- $\rho(r_i)$ is the expected density in the i-th spherical shell,
- M_i is the expected mass in the shell, given by:

$$M_i = \frac{N}{(2\pi\sigma^2)^{3/2}} \int_{r_{i-1}}^{r_i} 4\pi r^2 \exp\left(-\frac{r^2}{2\sigma^2}\right) dr$$

- V_i is the volume of the shell:

$$V_i = \begin{cases} \frac{4}{3}\pi r_i^3 & \text{if } i = 0 \\ \frac{4}{3}\pi(r_i^3 - r_{i-1}^3) & \text{if } i > 0 \end{cases}$$

We obtain the following graph which matches very closely to the expected density distribution.

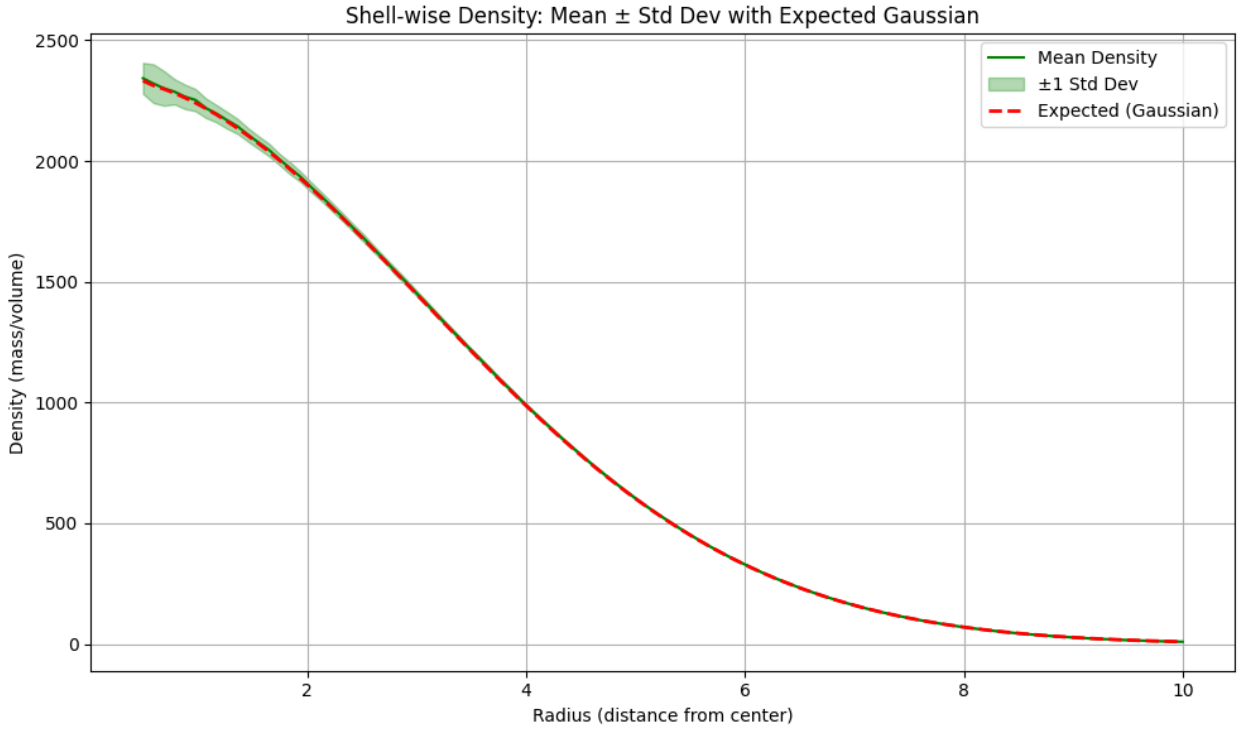

Figure 5: Error Analysis for Gaussian Distribution

To get a better idea of the density profile we will once again plot the over-density with the radius given by the same formula.

$$\delta(r) = \frac{\rho(r) - \bar{\rho}}{\bar{\rho}}$$

where:

- $\delta(r)$ is the overdensity at radius r,
- $\rho(r)$ is the spherically integrated (average) density within radius r,
- $\bar{\rho}$ is the average density of the entire volume:

$$\bar{\rho} = \frac{M_{\text{total}}}{V_{\text{total}}}$$

The same reasoning for shot noise is valid for this as well.

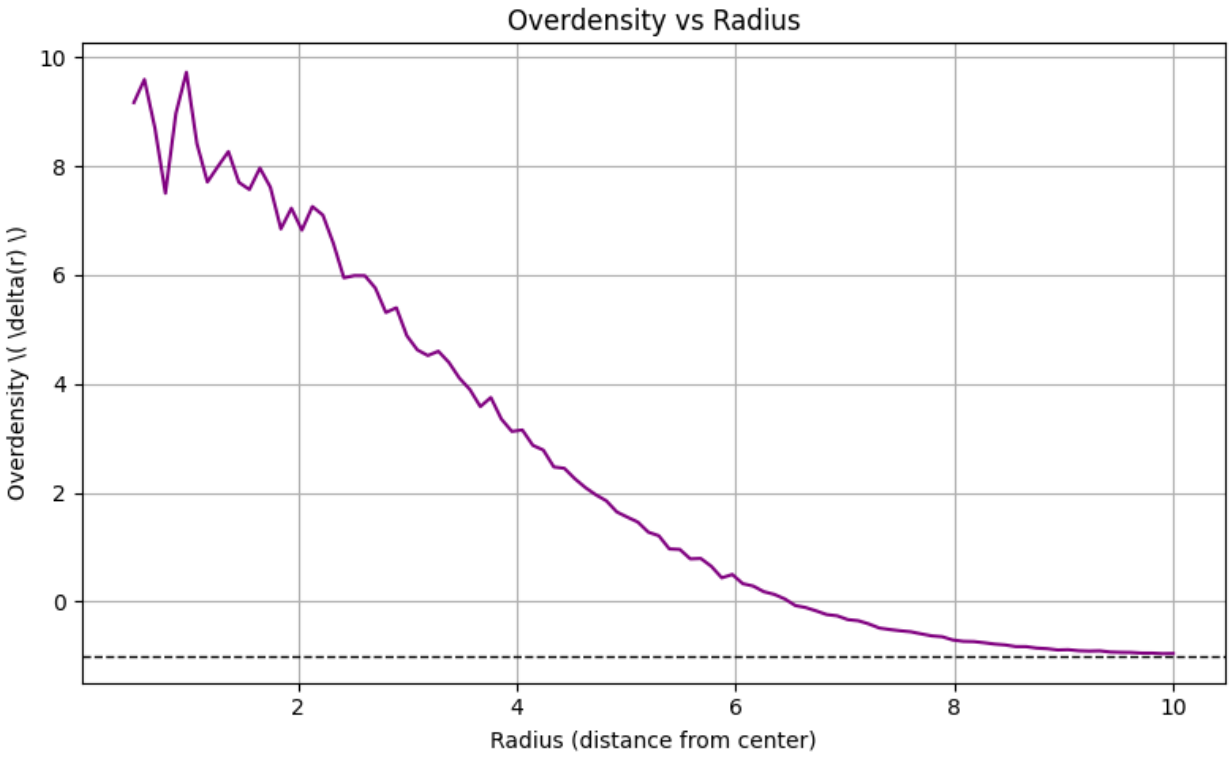

Figure 6: Overdensity Plot

3 Simulation Analysis

Using 2 files on the github repository of the simulation particularly - **out_200.trees** and **snapshot_200.hdf5** we identify the primary halos that are useful for us and then extract the number of point masses that exist within that particular halo.

3.1 Halo Identification

The file `out_200.trees` contains a wealth of information about halos identified in the simulation. Some of the key physical properties recorded for each halo include:

- **Virial Mass** (`Mvir`) – the total mass within the virial radius.
- **Virial Radius** (`Rvir`) – the radius enclosing the virial mass.
- **Scale Radius** (`rs`) – the characteristic radius from NFW profile fitting.
- **Maximum Circular Velocity** (`Vmax`) – the peak of the circular velocity curve.
- **Velocity Dispersion** (`vrms`) – a measure of the internal random motion of particles.
- **Position** (`x, y, z`) – the center of the halo in comoving coordinates.
- **Center-of-Mass Velocity** (`vx, vy, vz`) – the bulk velocity of the halo.
- **Angular Momentum** (`Jx, Jy, Jz`) – the total angular momentum vector of the halo.

We assumed a certain mass threshold = 10^{14} and filtered all the haloes based off of it, that is, consider only the halos that are above the mass threshold.
This gave us the following halos that meet our criteria :

Mvir	Rvir	x	y	z	vx	vy	vz
9.243	1976.273	189.25	136.15	120.90	276.29	-72.89	-23.05
6.868	1789.999	178.82	111.75	23.02	345.16	-75.54	362.27
6.476	1755.210	198.29	16.61	43.09	42.14	-398.44	-47.94
5.866	1698.362	8.12	135.75	83.85	-220.10	206.76	206.37
5.585	1670.795	149.33	174.44	99.42	55.66	-243.98	-193.63

Table 1: Virial mass, virial radius, position, and velocity components of selected halos.

3.2 Determining Points inside Halo

For this part we will only choose a halo from those detected, the one with **Mvir** = 9.243 and perform the calculation for it.
This halo has the following properties : The second file **snapshot_200.hdf5** has the information about

Property	Value
M_{vir}	$9.243\,M_{\odot}/h$
R_{vir}	$1976.273\,\text{kpc}/h$
x	$189.24596\,\text{Mpc}/h$
y	$136.15475\,\text{Mpc}/h$
z	$120.90205\,\text{Mpc}/h$
v_x	$276.29\,\text{km/s}$
v_y	$-72.89\,\text{km/s}$
v_z	$-23.05\,\text{km/s}$

Table 2: Properties of the selected dark matter halo.

various points in the numerical simulation, particularly their centre of mass and velocities. Assuming the halo to be a sphere with radius equal to virial Radius, we can check which points lie within the halo using a mask and we get the following :

```
Number of particles within radius: 131657
First 5 positions:
[[189.25424  136.34824  120.88043 ]
 [189.23906  136.35173  120.860435]
 [189.24187  136.37282  120.87555 ]
 [189.21852  136.36864  120.86115 ]
 [189.22015  136.36383  120.86505 ]]
First 5 velocities:
[[-331.90327744 -708.06733643 1205.3501709 ]
 [  14.22983643 -508.4672998   401.73969727]
 [1144.71427246  176.55889191 -170.10841675]
 [ 572.64530273  701.0596167  -924.98875732]
 [1133.83158203 -333.49882446  -54.72059174]]
```

Figure 7: List of points within a Halo

4 Density Calculation

Now that we have the various points within the halo, we create bins of varying radius to calculate the density of each concentric shell. We divide the total radial distance logarithmically, starting from a minimum value of 10^{-2} Mpc up to the virial radius. We know the mass of each particle in the simulation is equal to 4.15153252 $M_{\odot}$, so we can easily compute the density of each shell as follows: first, we count the number of particles within each radial shell. Then, we multiply this count by the mass per particle to obtain the mass contained in each shell. Finally, we divide the mass of each shell by its corresponding volume to obtain the density:

$$\rho_i = \frac{N_i \times m_{\text{particle}}}{\frac{4}{3}\pi\left(r_{i+1}^3 - r_i^3\right)}$$

where N_i is the number of particles in the i^{th} shell, m_{particle} is the mass of each particle, and r_i, r_{i+1} are the inner and outer radii of the shell respectively.
Using the above formula we get the following graph for the density plot, both the axes are in logarithmic scale.

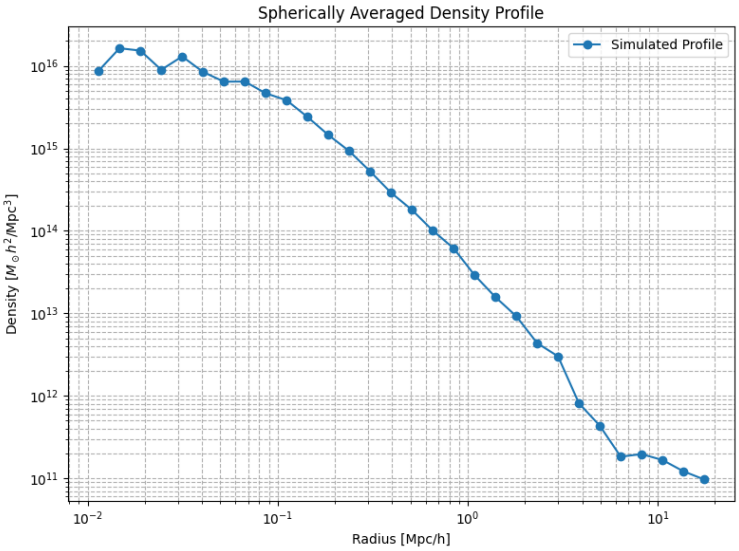

Figure 8: Density Plot for Halo 1

5 Plots for various Halos

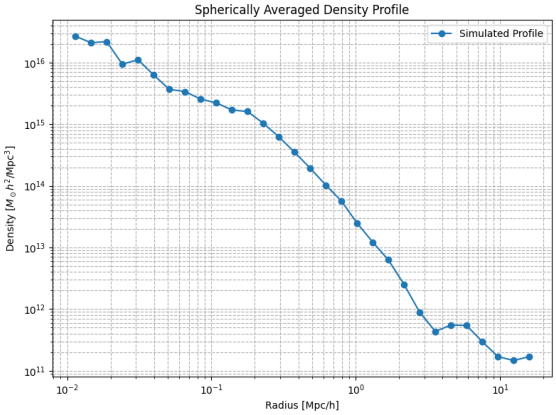

(a) Halo 2

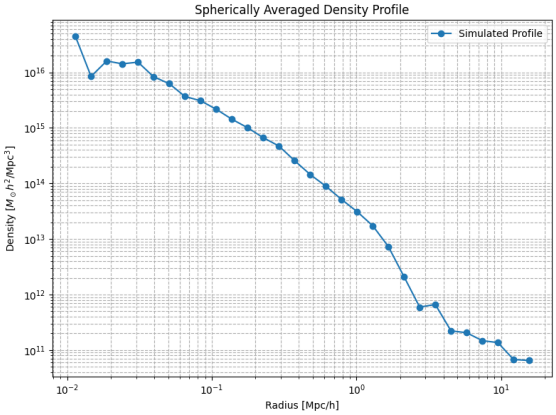

(b) Halo 3

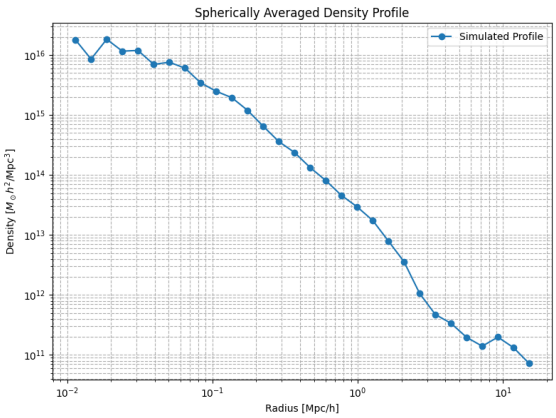

(c) Halo 4

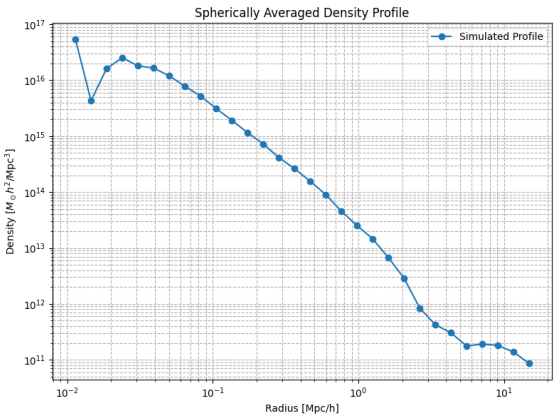

(d) Halo 5

Figure 9: Spherical density profiles for the remaining Halos.

6 Fitting the NFW Profile

The Navarro-Frenk-White (NFW) profile is a standard analytical model used to describe the spherically averaged density distribution of dark matter halos. It is given by:

$$\rho(r) = \frac{\rho_s}{\left(\frac{r}{r_s}\right)\left(1+\frac{r}{r_s}\right)^2}, \tag{3}$$

where ρ_s is a characteristic density and r_s is a scale radius. This profile exhibits a central cusp ($\rho \propto r^{-1}$ as $r \to 0$) and falls off as r^{-3} at large radii, matching predictions from ΛCDM cosmological simulations.

To fit the NFW profile to the simulated halo data, we first computed the radial density profile from the simulation. Since densities span several orders of magnitude, we transformed the data into logarithmic space to stabilize the fitting process and reduce numerical sensitivity. Only valid points—those with positive, finite density—were considered during the fit.

A nonlinear least-squares optimization was performed to determine the best-fit values of ρ_s and r_s. The fitted profile was then evaluated over a smooth range of radii and plotted alongside the original simulation data.

The resulting fit parameters were:

- $\rho_s = 1.314 \times 10^{15}\,\mathrm{M_\odot h^2/Mpc^3}$
- $r_s = 0.183\,\mathrm{Mpc/h}$

The fitted NFW curve showed excellent agreement with the simulated density profile across the radial range, capturing both the inner cusp and the outer decline. The comparison is illustrated in Figure 10.

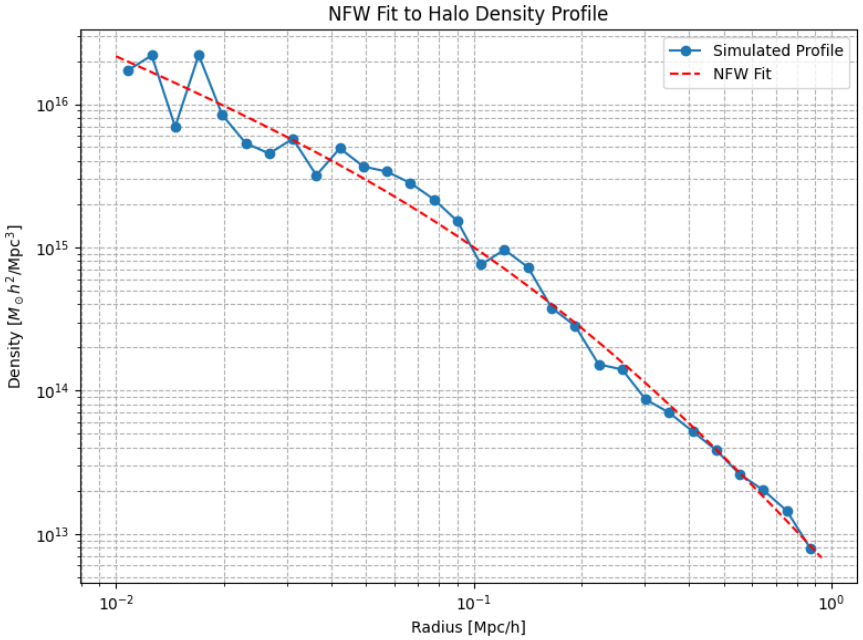

Figure 10: Halo density profile from simulation (dots) compared with the best-fit NFW model (dashed line).

7 Overdensity Calculation and Comparison

The overdensity contrast $\delta(r)$ quantifies the deviation of the local matter density $\rho(r)$ from the mean matter density of the Universe $\bar{\rho}$ and is defined as:

$$\delta(r) = \frac{\rho(r) - \bar{\rho}}{\bar{\rho}}. \tag{4}$$

To compute this, we first evaluate the critical density of the Universe using:

$$\rho_{\mathrm{crit}} = \frac{3H_0^2}{8\pi G}, \tag{5}$$

where H_0 is the Hubble parameter and G is Newton's gravitational constant. Assuming a flat ΛCDM cosmology with $\Omega_m = 0.3$, the mean matter density is given by:

$$\bar{\rho} = \Omega_m \rho_{\mathrm{crit}}. \tag{6}$$

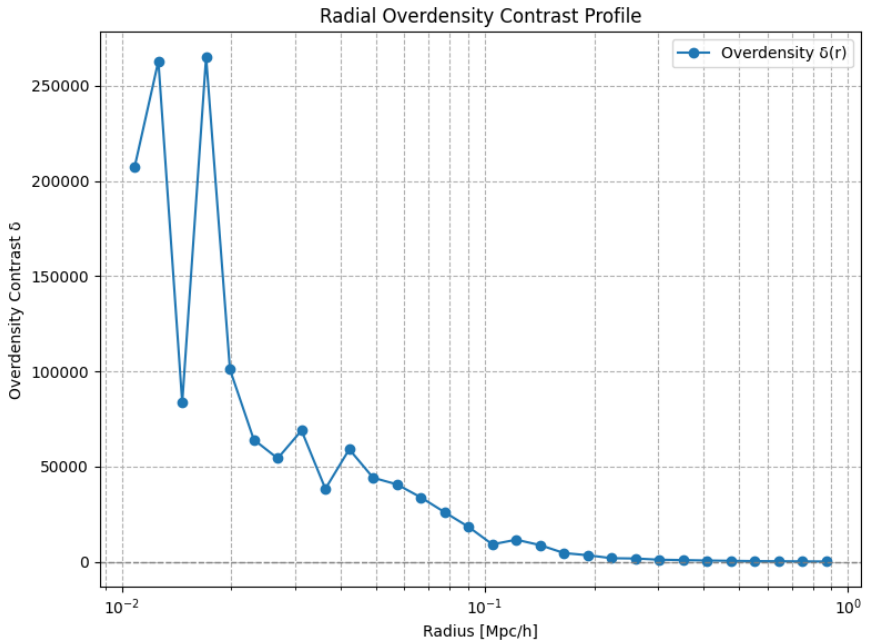

Figure 11: Radial overdensity contrast $\delta(r)$ calculated from the simulation.

Using the radial density profile from the simulation, the overdensity contrast was computed at each radial bin. Figure 11 shows the radial profile of $\delta(r)$ derived from the simulation data.

To assess the accuracy of the fitted NFW model, we also computed the overdensity contrast using the NFW density profile:

$$\delta_{\mathrm{NFW}}(r) = \frac{\rho_{\mathrm{NFW}}(r) - \bar{\rho}}{\bar{\rho}}. \tag{7}$$

This provides a direct comparison between the simulation and the analytical model in terms of their departure from the cosmic mean density. As shown in Figure 12, the simulated and NFW overdensity profiles agree well over most radial ranges, with slight deviations at small and large scales.

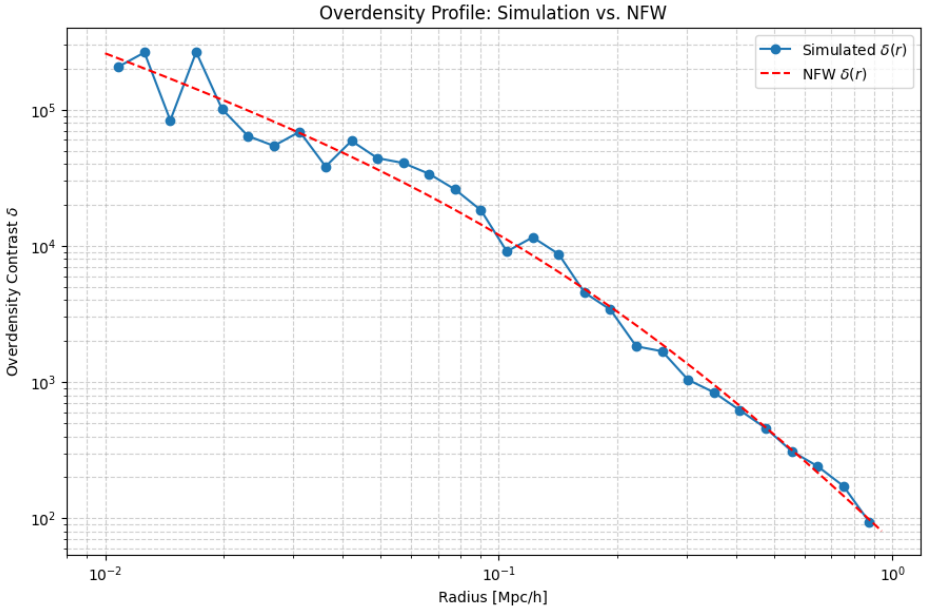

Figure 12: Comparison of the overdensity contrast $\delta(r)$ from the simulation and the best-fit NFW model.

8 Velocity Profile Analysis

To characterize the kinematic structure of the dark matter halo, we analyzed the particle velocity distribution in both Cartesian and spherical coordinates. This analysis reveals coherent bulk motions, infall patterns, and anisotropies in the velocity field.

8.1 Cartesian Velocity Components

We first extracted the Cartesian velocity components v_x, v_y, and v_z of all particles and computed their average values in logarithmically spaced radial bins centered around the halo. The mean velocities along each axis were computed as a function of radius using:

$$\langle v_i(r) \rangle = \frac{1}{N_r} \sum_{j \in \text{bin}(r)} v_i^{(j)}, \quad i \in \{x, y, z\}, \tag{8}$$

where N_r is the number of particles in the radial bin. These average velocities are plotted in Figure 13, showing how the net motion varies across the halo.

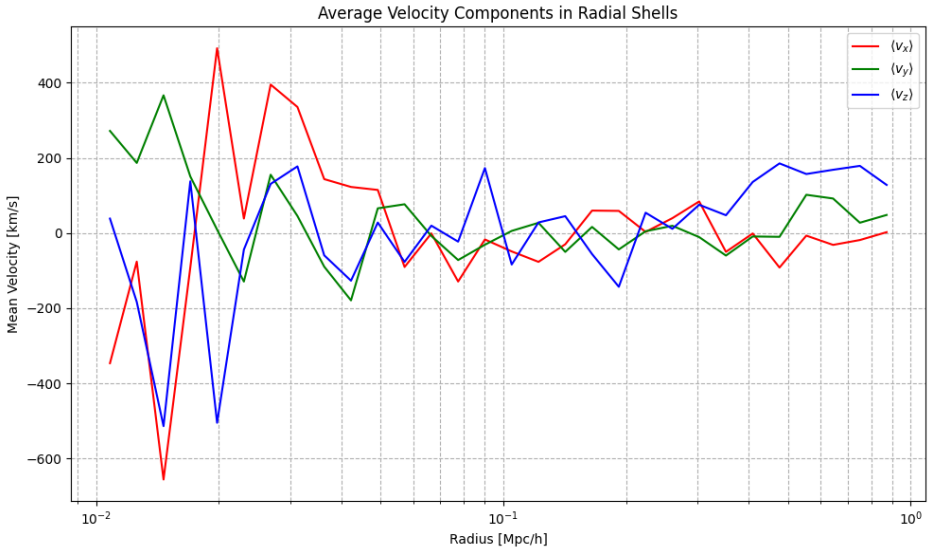

Figure 13: Average Cartesian velocity components as a function of radius.

8.2 Spherical Velocity Components

To gain a more physically meaningful interpretation of particle motions, we transformed the velocity vectors into spherical coordinates. The radial (v_r), polar (v_θ), and azimuthal (v_ϕ) components were computed by projecting the 3D velocity vectors onto the local spherical basis vectors defined at each particle's position:

$$v_r = \vec{v} \cdot \hat{r}, \tag{9}$$

$$v_\theta = \vec{v} \cdot \hat{\theta}, \tag{10}$$

$$v_\phi = \vec{v} \cdot \hat{\phi}. \tag{11}$$

The magnitudes of these components were then averaged in the same radial bins used for the density profile. Figure 14 shows the radial dependence of the spherical velocity components. The radial component dominates at large radii, indicating infall motion, while the tangential components exhibit varying behavior, revealing the presence of angular momentum and velocity anisotropies.

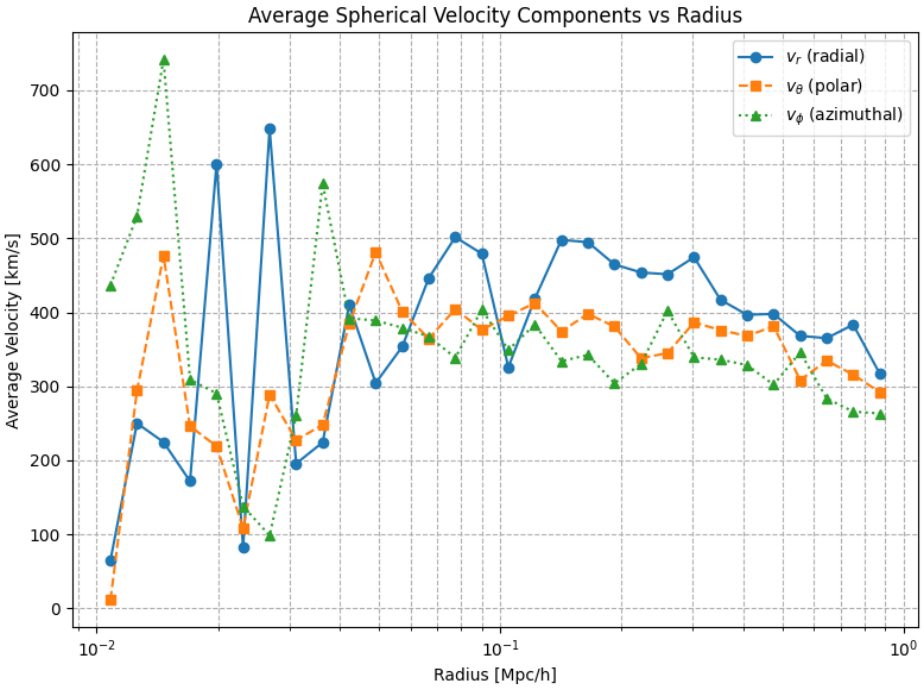

Figure 14: Average spherical velocity components (v_r, v_θ, v_ϕ) as a function of radius.

9 Conclusion

In this study, we successfully analyzed the radial density distribution of a simulated dark matter halo and demonstrated that it is well-described by the Navarro-Frenk-White (NFW) profile. By computing the critical and mean matter densities, we derived the radial overdensity contrast $\delta(r)$, which provided a physically meaningful measure of how the halo deviates from the cosmological background. The excellent agreement between the simulation data and the NFW model confirms the reliability of the halo identification and density estimation procedures.

On the other hand, our investigation of the velocity structure remains incomplete. While the average Cartesian and spherical velocity components were computed as a function of radius, the results revealed unexpected behavior—particularly, the radial velocity component v_r did not dominate at large radii as typically expected for halos undergoing infall. This deviation may indicate the presence of significant angular momentum or internal rotational support, suggesting that the halo may possess a non-negligible spin.

Further analysis will focus on extending this study to a larger ensemble of halos in order to investigate whether the suppressed radial velocity component v_r is a general feature or specific to this particular system. Comparing halos across a range of masses, spins, and environments may reveal consistent trends or anomalies in their kinematic structure. Additionally, we will consider the framework of the ellipsoidal (or elliptical) collapse model, which accounts for anisotropic gravitational collapse and tidal torques, to better interpret deviations from the spherical infall expected in the standard model. These investigations will help clarify whether the observed velocity behavior arises from intrinsic halo properties or from more complex dynamical processes.